Synthesis of Anion Electrolyte Membrane through Radiation-induced Graft Polymerization of Poly(4-vinylbenzyl chloride) onto Isotactic Polypropylene Film

Patrick Jay E. Cabalar[1*], Takashi Hamada[2, 3],
Jordan F. Madrid[1] and Noriaki Seko[2]

[1]Chemistry Research Section
Department of Science and Technology – Philippine Nuclear Research Institute
(DOST-PNRI), Quezon City, 1101 Philippines
*pjecabalar@pnri.dost.gov.ph

[2]Takasaki Advanced Radiation Research Institute
National Institute for Quantum Radiological Science and Technology
Takasaki, Gunma 370-1292 Japan

[3]Graduate School of Advanced Science and Engineering
Hiroshima University
Higashi-Hiroshima, Hiroshima 739-8527 Japan

Abstract

Radiation grafting, a widely used process for preparing different functional materials, allows the facile amalgamation of desirable properties from two or more polymers without altering the inherent properties of the base substrate. In this study, an anion electrolyte membrane (AEM) was successfully prepared through radiation grafting of poly(vinylbenzyl chloride) (PVBC) from isotactic polypropylene (iPP) film using gamma-ray irradiation. It was shown that the amount of grafted PVBC increased with increasing absorbed dose, which yielded iPP-g-PVBC with 127% degree of grafting at 50 kGy. The iPP-g-PVBC was reacted with aqueous trimethylamine hydrochloride solution to introduce quaternary ammonium ions, thereby producing the AEM membrane in chloride form (iPP-g-PVBC-TMA-Cl), which was further reacted with potassium hydroxide (KOH) to convert it into hydroxide form (iPP-g-PVBC-TMA-OH). The pristine, grafted and functionalized iPP films were characterized using attenuated total reflectance – Fourier transform infrared spectrometer, thermogravimetric analyzer and scanning electron microscopy – energy dispersive X-ray spectrometer. The effect of degree of grafting on the ionic conductivity, ion exchange capacity and water uptake were evaluated in both AEM's chloride and hydroxide forms. Results showed that a higher degree of grafting films achieved higher ionic conductivity, ion exchange capacity and water uptake for both chloride and hydroxide forms. The synthesized AEM with a degree of grafting of 70% (IEC = 1.87 meq/g) obtained a conductivity of 129.34 mS/cm, which is higher than the AEMs reported in previous works.

Keywords: anion exchange membrane, conductivity, fuel cells, polypropylene, radiation-induced graft polymerization

1. Introduction

Technological advancements have paved the way for the introduction of alternative energy systems (e.g., fuel cell systems [FCS] that convert fuel's stored chemical energy into electrical one [Page and Rowe, 2012]) to mobile and portable devices, thereby replacing or complementing petroleum-based energy systems. Although commonly used in industrial applications (i.e., mobile and stationary energy devices) (Sherazi *et al*., 2013), FCS can be utilized as temporary devices during natural disasters. Hence, this is particularly helpful in the Philippines, which is frequently hit by typhoons. Owing to the benefits of FCS, a Philippine telecommunications company has started to deploy FCS in its cellular telecom sites as backup power systems in lieu of diesel-powered generator sets (Fuel Cells Bulletin, 2021).

Early popular fuel cell assemblies used platinum (Pt) as electrodes. Acidic solutions, such as dilute sulfuric acid, were frequently utilized as electrolytes (Page and Rowe, 2012). At the turn of the century, there has been an increased interest in polyelectrolyte membranes research for fuel cell applications as manifested by the increasing number of research publications in the early 2000s (Page and Rowe, 2012). There are various types of membranes used in polymer electrolyte membrane fuel cells (PEMFCs). The most common ones are proton exchange membranes (PEMs) and anion exchange membranes (AEMs).

PEMs contain negative ionic groups or proton conducting groups, while AEMs constitute positive ionic groups and mobile anions like hydroxide ion (OH-) (Espiritu *et al*., 2016). On one hand, PEMs are promising; however, the adoption is limited due to its relatively high cost (Sherazi *et al*., 2013) and reliance on expensive metal catalysts such as Pt (Couture *et al*., 2011; Sherazi *et al*., 2013). On the other hand, AEMs have lower dependence on noble metal catalysts compared with PEMs (Sherazi *et al*., 2013; Espiritu *et al*., 2016). In AEM fuel cells (AEMFCs), non-noble metal catalysts such as nickel (Ni) and silver (Ag) can be used (Varcoe *et al*., 2006), thus reducing the cell's cost (Sherazi *et al*., 2013). AEMs also offer faster oxygen reduction reaction kinetics, and ion transport osmotic drag opposes the crossover of liquid fuels (Couture *et al*., 2011; Espiritu *et al*., 2016). Aside from its advantages over PEMs, AEMs' development addresses challenges on the use of alkaline fuel cells and replaces liquid electrolytes (Iojoiu *et al*., 2006).

AEMFCs work by using different fuels like hydrogen gas, methanol and sodium borohydride (Arges *et al*., 2010). The fuel is oxidized at the anode and reacts with the hydroxide ions that are transported through the electrolyte membrane from the cathode and consequently produce water (Mahmoud and Güven, 2012; Dekel, 2018; Ramirez and Paz, 2018). The produced water through the reaction leaves the cell while some move through the electrolyte membrane to the cathode. The electrons, obtained via the fuel oxidation process, transport from an external circuit to the cathode, wherein they undergo oxygen gas reduction to form hydroxide ions (Arges *et al*., 2010).

The radiation-induced graft polymerization (RIGP) technique is a commonly used process for improving polymer without changing its inherent properties (Dargaville *et al*., 2003). It does not employ chemicals in the free radical formation initiation; thus, the purity of the resulting product is maintained (Bhattacharya and Misra, 2004; Sherazi *et al*., 2008; Pomicpic *et al*., 2020). RIGP has also been employed in synthesizing heavy metal ion adsorbents (Seko *et al*., 2007; Madrid and Abad, 2015; Madrid *et al*., 2018; Lopez *et al*., 2020), precious metal recovery (Hoshina *et al*., 2014), biodiesel catalyst (Ueki *et al*., 2014) and dye adsorbent (Pomicpic *et al*., 2020). Additionally, RIGP has been utilized in producing polymer electrolyte membranes using different polymer backbones, namely polyethylene (Sherazi *et al*., 2013; Espiritu *et al*., 2016), poly(ethylene-co-tetrafluoroethylene) (Varcoe and Slade, 2006; Laura *et al*., 2018), poly(ether ether ketone) (Zhang, 2019), polybenzimidazoles (Park *et al*., 2013) and poly(2,6-dimethyl-1,4-phenylene oxide) (Yang *et al*., 2019).

Polypropylene (PP) has excellent chemical and high-temperature resistance and dimensional stability. PP has different stereo-specific configurations depending on the arrangement of the methyl groups: isotactic (placement of methyl groups on one side), syndiotactic (alternation of methyl groups on both sides) and atactic (irregular arrangement of the methyl groups) (Maddah, 2016). Among these three configurations, only the isotactic and syndiotactic forms can create a polycrystalline structure with acceptable physical and tensile properties (Ghosh, 1998). Isotactic polypropylene (iPP) has a higher melting point of 171 °C compared with the syndiotactic PP (melting point: 130 °C) (Maddah, 2016). These characteristics, combined with its high market availability, qualify iPP as a good backbone for an AEM.

This work reports for the first time the preparation of an anion electrolyte membrane (AEM) from an iPP substrate through RIGP via pre-irradiation technique. The overall synthesis process is illustrated in Figure 1.
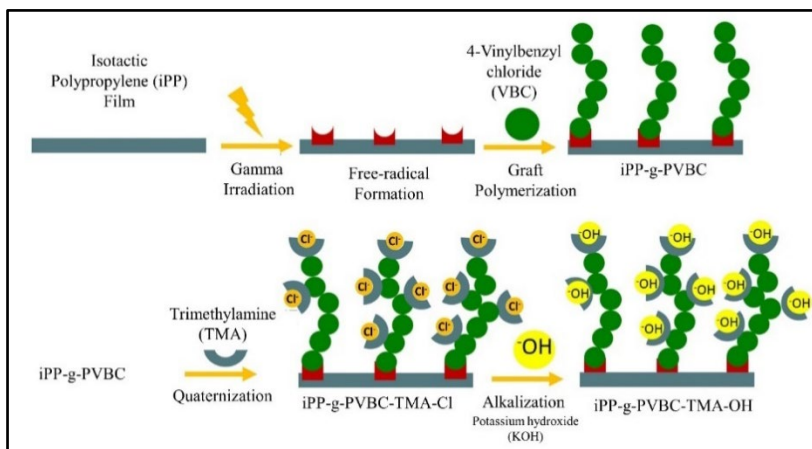

Figure 1. Synthesis of iPP-based AEM via RIGP

The prepared iPP films were irradiated using gamma-ray at different absorbed doses to form free radicals on the surface and in the film's bulk. The vinylbenzyl chloride (VBC) was graft-polymerized from the irradiated iPP film that formed iPP-g-PVBC. The iPP-g-PVBC was quaternized using trimethylamine (TMA) forming the iPP-g-PVBC-TMA-Cl (chloride form) followed by alkalization, which formed the iPP-g-PVBC-TMA-OH (hydroxide) AEM. The pristine film, iPP-g-PVBC, iPP-g-PVBC-TMA-Cl and iPP-g-PVBC-TMA-OH were characterized using attenuated total reflectance – Fourier-transform infrared spectroscopy (ATR-FTIR), scanning electron microscopy – energy-dispersive X-ray spectroscopy (SEM-EDX) and thermogravimetric analysis (TGA). The effect of absorbed dose on the degree of grafting and the effect of degree of grafting on the degree of amination, amine group density (AGD), ion exchange capacity, water uptake and ionic conductivities was systematically investigated.

2. Methodology

2.1 Materials

The iPP pellets (MW = ~340,000) and VBC monomer were purchased from Sigma-Aldrich (United States) and AGC Seimi Chemical Co., Ltd. (Japan),

respectively. Polyoxyethylene (20) sorbitan monolaurate (Tween 20) was used as a nonionic surfactant in the preparation of the monomer emulsion, TMA (30% in water), potassium hydroxide (KOH) (86%), 1M aqueous hydrochloric acid standard solution (Kanto Chemical Co., Inc., Japan). Toluene (99.0%), methanol (technical grade) and sodium hydroxide were supplied by Wako Pure Chemical Industries, Ltd. (Osaka, Japan). Acetone (HPLC grade) was obtained from Aldrich (United States). Deionized water filtered from the Milli-Q deionization system with a resistance of 15.0 MΩ was used for the preparation of aqueous solutions.

2.2 Synthesis of iPP-g-PVBC-TMA-OH AEM

2.2.1 Preparation of iPP films

Approximately 2 g of iPP pellets were melt-pressed into films using a hot press (IKEDA, Japan) at a set plate temperature of 200 °C for 15 min at 150 kg/m^2 pressure and cooled down using the cold press (Toyo Seiki, Japan). This produced films with 50- to 70-um average thickness. Film thickness was measured using a digital caliper (Mitutoyo, Japan). The prepared films had been washed with methanol and dried before they were utilized in the succeeding experiments.

2.2.2 Irradiation and Grafting

The iPP film was cut into 3 x 3 cm square pieces and the initial weight was recorded. The film was washed with methanol and dried in vacuo at 35 °C for 24 h before irradiation. After drying, the film was placed in a polyethylene (PE) resealable bag. The samples were purged with nitrogen gas (N$_2$) (g) to remove air in the system prior to irradiation. The samples were irradiated at the [60]Co Gamma Irradiation Facility (Takasaki Advanced Radiation Research Institute, Japan) at absorbed doses ranging from 10 to 50 kGy with an increment of 10 kGy and at a dose rate of 10 kGy/h.

After irradiation, the irradiated iPP samples were placed in reaction ampoules, then deaerated before it was filled with an aqueous emulsion containing VBC and Tween 20. The graft polymerization reaction was carried out at 60 °C for 5 h in a thermostatic water bath. Afterward, the samples were washed with toluene and acetone to remove unreacted VBC and ungrafted homopolymers. The synthesized iPP-g-PVBC samples were oven-dried overnight in vacuo at 35 °C. The degree of grafting (%) was determined gravimetrically and calculated using Equation 1.

$$Degree\ of\ grafting\ (\%) = \frac{W_f - W_i}{W_i} \times 100 \qquad (1)$$

where W_i and W_f are the measured weights of the pristine iPP film and the measured weight of the iPP-g-PVBC, respectively.

2.2.3 Quaternization and Alkalization

The iPP-g-PVBC membranes were reacted with 1M aqueous TMA solution at 40 °C for 24 h. After amination, the membranes were washed with deionized water then with 1M HCl to remove excess TMA and lastly with deionized water. The quaternized membranes, denoted as iPP-g-PVBC-TMA-Cl, were dried overnight in vacuo at 35 °C. The quaternized weight was measured through weighing by difference. Lastly, the iPP-g-PVBC-TMA-Cl membranes were reacted with nitrogen-purged 1M KOH for 12 h to introduce hydroxide ions by exchanging with the chloride counter-ions. The samples were washed with N_2-purged deionized water and dried overnight in vacuo at 35 °C. After drying, the alkalized weight of the membranes was measured through weighing by difference.

The degree of amination (Da) (%) and amine group density (AGD) (mmol/g catalyst) were calculated using Equations 2 and 3, respectively.

$$Da\ (\%) = \left[\frac{MW_{VBC} \times \frac{(W_q - W_f)}{(W_f - W_i)} - MW_{VBC}}{MW_{TMA}} \right] \times 100 \qquad (2)$$

$$AGD \left(\frac{mmol_{amine}}{g\ catalyst} \right) = \frac{W_q - W_f}{W_q} \times \frac{1000}{MW_{TMA}} \qquad (3)$$

where W_i, W_f, W_q, MW_{VBC} and MW_{TMA} are the weights of the pristine iPP, aminated iPP-g-PVBC, iPP-g-PVBC-TMA-Cl and molecular weights of the VBC monomer and TMA, respectively.

2.3 Membrane Characterization

FTIR was performed using an IR spectrometer (Perkin Elmer Frontier, United Kingdom) equipped with ATR accessory (Czitech MicromATR Vision, S.T. Japan Inc., Japan) in the range of 4,000-400 cm^{-1} and resolution of 4 cm^{-1}. The thermal degradation behavior and thermal stability analyses were done using

a thermogravimetric analyzer (ThermoPlus [TG 8120], Rigaku, Japan) from 100 to 700 °C at a heating rate of 10 °C/min under nitrogen atmosphere (100 L/min). Pre-heating at 100 °C for 1 h was employed to remove the adsorbed water molecules. The morphology of the samples was observed using a scanning electron microscope (SEM) (SU3500, Hitachi, Japan) equipped with an ultra-variable pressure detector (UVD). Images were taken at 5 kV accelerating voltage and 50 Pa pressure in a vacuum. The elemental distribution profiles of chlorine, carbon and oxygen in the cross-section of the AEMs were measured using an energy dispersive X-ray spectrometer (EDX) (X-Max^N, HORIBA, Japan).

2.4 Ionic Conductivities

2.4.1 Chloride Ion Conductivity

The iPP-g-PVBC-TMA-Cl membranes with varying degrees of grafting were hydrated in N_2-purged deionized water in a sealed container for 1 h before the conductivity analysis. Each membrane was tested at 25 and 60 °C. The 60 °C setup was done in a thermostatic water bath. The membrane was sandwiched between two plates, while the membrane distance, membrane thickness and membrane length were recorded. The plate assembly containing the membrane sample was submerged in a beaker containing N_2-purged water. It was allowed to equilibrate until a stable impedance (Ω) reading was observed in the rheometer (IM 3523, HIOKI, Japan) with +/– 0.05 accuracy. The ionic conductivity (IC) was calculated using Equations 4 and 5.

$$\sigma = \frac{l \times 10^3}{S \times R} \tag{4}$$

$$S = d \times t \tag{5}$$

where σ, S, R, d, t and l are the IC (mS/cm), area of the membrane between the electrodes (cm^2), impedance (Ω), membrane distance (cm), membrane thickness (cm) and membrane length (cm), respectively.

2.4.2 Hydroxide Ion Conductivity

The iPP-g-PVBC-TMA-OH membranes were first washed with N_2-purged deionized water for 30 min. N_2-purging of deionized water significantly decreases the dissolved CO_2, which could react with the hydroxide ions on the membrane, leading to a decrease in IC, thus affecting the overall performance of the intended fuel cell (Zheng *et al.*, 2021). The washing process was

performed three times. The ionic conductivities were then measured following the procedure in section 2.4.1.

2.5 Water Uptake (WU)

The chloride and hydroxide forms of the AEMs were immersed in N_2-purged deionized water for 24 h. The percentage WU was determined by measuring the weight difference before and after immersion (Equation 6).

$$WU\ (\%) = \frac{W_{wet} - W_{dry}}{W_{dry}} \times 100 \qquad (6)$$

where W_{dry} and W_{wet} are the dry and hydrated weight of the membrane, respectively.

2.6 Ion-Exchange Capacity (IEC) Measurements

The IEC is the number of cation groups present in the membrane that are available for exchange with OH- ions per mass unit of dry membrane; they are expressed as meq/g dry membrane (Merle *et al*., 2011; Lim *et al*., 2015; Espiritu *et al*., 2016). The IEC of the iPP-g-PVBC-TMA-OH membranes with varying degrees of grafting was determined through the titration method (Espiritu *et al*., 2016). The membranes were thoroughly washed with N_2-purged deionized water before immersing in individual containers containing 0.1M HCl. The setups for IEC were allowed to equilibrate for 24 h. The membranes were removed and the solution was titrated with 0.1M NaOH standard solution using an automatic titrator (COM-2000, HIRANUMA, Japan) with burette (B-2000, HIRANUMA, Japan). The IEC of the membranes was calculated using Equation 7.

$$IEC\ (\frac{meq}{g}) = \frac{(V_{ref} - V_{mem}) \times C_{NaOH}}{W_{dry,OH}} \qquad (7)$$

where V_{ref}, V_{mem}, C_{NaOH} and $W_{dry,OH}$ are the volume required for the neutralization of the reference solution (0.1M HCl), volume necessary for the neutralization of the residual solution, the concentration of the sodium hydroxide titrant and the dry weight of the AEMs in hydroxide form, respectively.

3. Results and Discussion

3.1 Effect of Absorbed Dose on Degree of Grafting

Various iPP-g-PVBC with different degrees of grafting values were prepared and the results are presented in Figure 2.
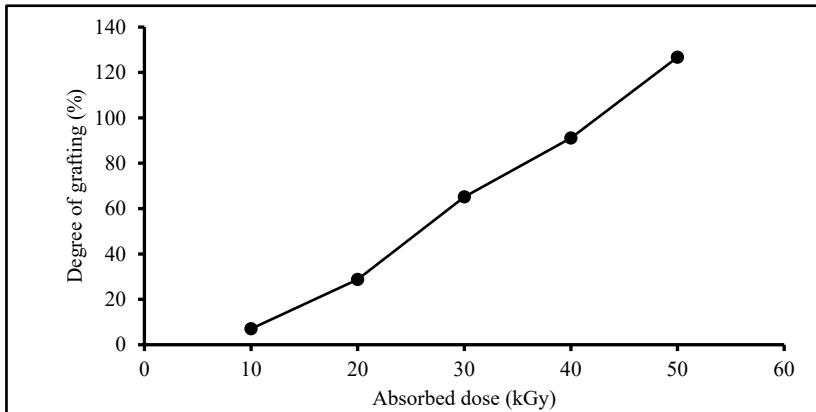

Figure 2. The effect of absorbed dose on degree of grafting

It was observed that the degree of grafting increased with increasing absorbed dose with the highest average degree of grafting value of 127% recorded at 50 kGy. This trend was due to the increased formation of free radicals on the iPP film that increased the number of possible reaction sites for the graft polymerization process (Pomicpic *et al.*, 2020). Albano *et al.* (2006) studied the effect of irradiation on polyethylene (PE)/polyamide (PA) blends, and the results showed that the free radical concentration increased with increasing absorbed dose up to 800 kGy and the same effect was observed even in irradiated pure PA and PEs with low, linear low and high densities. Total free radical concentration also increased with increasing absorbed dose of irradiated polypropylene (PP) and its blends with styrene-butadiene-styrene (SBS) from 0 to 100 kGy (Madrid *et al.*, 2016). The desired degree of grafting for fuel cell and membrane applications is 20-50% (Bhardwaj *et al.*, 2014). In this study, the mentioned values were achieved at absorbed doses of 20-30 kGy. In previous work, membranes with degree of grafting values < 75% are suitable for fuel cell applications but must be > 35% to operate for a prolonged time at 50 °C and above temperatures (Espiritu *et al.*, 2016). The membranes with different degrees of grafting values were evaluated on different AEM performance parameters and the results are discussed in the succeeding sections.

3.2 Effect of Degree of Grafting on Da and AGD

The effect of different amounts of PVBC graft chains (i.e., the effect of degree of grafting on the Da and AGD) are shown in Figures 3 and 4, respectively. A lower degree of grafting values led to higher Da, as shown in Figure 3, mainly because the graft chains were not hindered and were readily available for reaction with TMA.
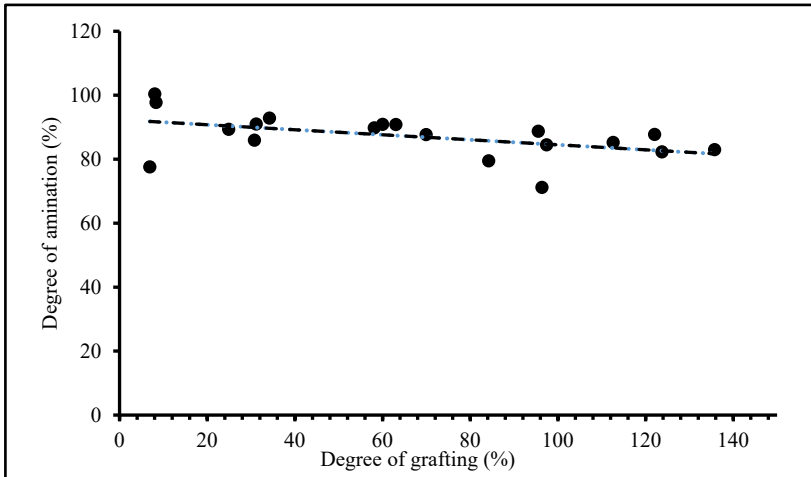

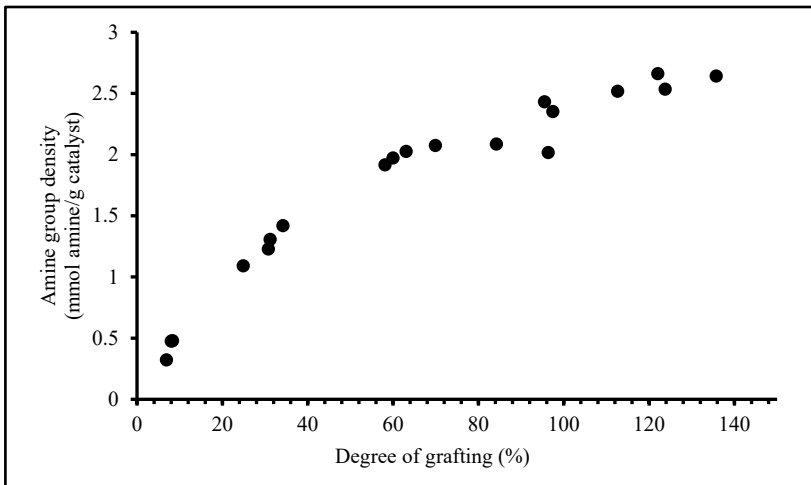Figure 3. Effect of degree of grafting on degree of amination

Figure 4. Effect of degree of grafting on amine group density

Consequently, films with a higher degree of grafting values exhibited a slight decrease in Da due to the higher amounts of grafted PVBC units. In terms of the AGD, an increasing degree of grafting values resulted in increased AGD with the highest attained from the film with a 136% degree of grafting. This trend was linked to more available sites for amination and quaternization in a higher degree of grafting films. In the samples, however, the AGD became almost constant beyond 120% degree of grafting (Figure 4). This could be due to non-accessible portions of the graft chains at a higher degree of grafting; denser brushes could hinder the diffusion of dissolved TMA. A high AGD grafted film is essential for an AEM because it has more sites for OH⁻ exchange, thereby creating a good conducting channel when used as an AEM in a fuel cell. Aside from AGD, other parameters must also be considered as shown in the next sections.

3.3 Characterization of AEMs

3.3.1 FTIR Spectra

Pristine iPP film, iPP-g-PVBC, iPP-g-PVBC-TMA-Cl and its alkalized form (iPP-g-PVBC-TMA-OH) were analyzed by ATR-FTIR to determine their chemical structures. The FTIR spectra results are shown in Figure 5.
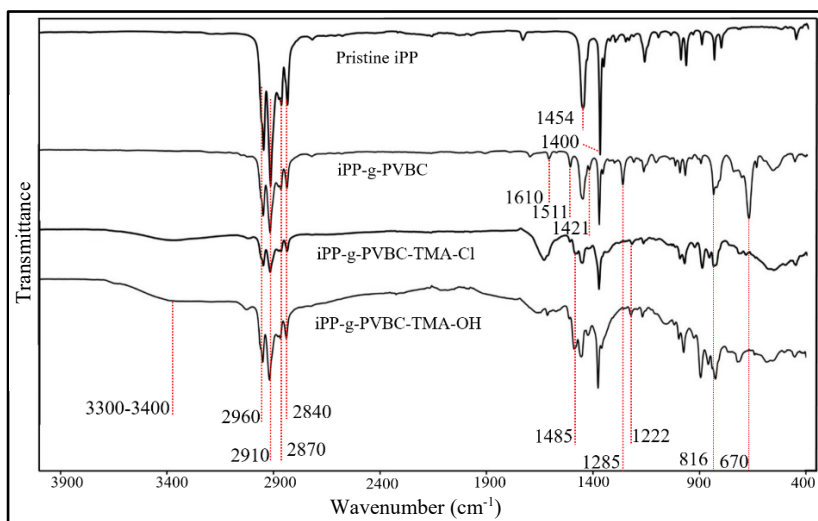

Figure 5. ATR-FTIR spectra of iPP film, iPP-g-PVBC,
iPP-g-PVBC-TMA-Cl and iPP-g-PVBC-TMA-OH

The peaks at 2,910-2,960 and 1,400-1,454 cm^{-1} corresponded to –CH2 asymmetric and symmetric stretching and –CH$_3$ bending (Espiritu *et al.*, 2016; Sherazi *et al.*, 2013) of the pristine iPP, respectively. The iPP-g-PVBC spectrum showed additional peaks at 1,421-1,610, 1,285, 816 and 670 cm^{-1} that can be attributed to the double bonds of the aromatic ring (Sherazi *et al.*, 2013; Espiritu *et al.*, 2016; An *et al.*, 2018), CH2-Cl wagging (Sherazi *et al.*, 2013), C-H deformation of the meta/para-substituted benzene ring (Espiritu *et al.*, 2016) and C-Cl stretching (Espiritu *et al.*, 2016), respectively. These peaks confirm the successful grafting of PVBC to the iPP film. The –CH2-Cl vibrational stretching peaks disappeared after the iPP-g-PVBC was quaternized with TMA, and new characteristic peaks appeared at 1,485 and 1,222 cm^{-1}, which corresponded to the quaternary ammonium ions (Sherazi *et al.*, 2008; Espiritu *et al.*, 2016; Zabbaruddin *et al.*, 2019) and symmetric C-N vibration (Sherazi *et al.*, 2008; Ueki *et al.*, 2011), respectively. In its alkalized form, the weak and broad peaked at 3,300-3,400 cm^{-1} is indicative of the O-H stretch and its successful incorporation to the quaternized membrane (Sherazi *et al.*, 2008).

3.3.2 Thermogravimetric (TG) Profile

The thermal stability of the PP film and synthesized membranes was determined using a TG analyzer and their degradation profiles are shown in Figure 6.
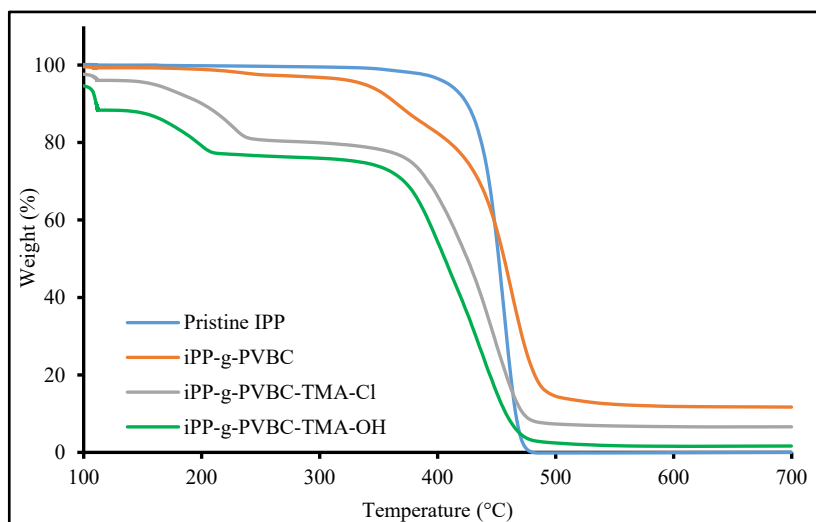

Figure 6. TG profiles of iPP film, iPP-g-PVBC, iPP-g-PVBC-TMA-Cl and iPP-g-PVBC-TMA-OH

The TG curve of the iPP film showed a single step weight loss in an inert atmosphere, which initiated at 350 °C before reaching a maximum weight loss at around 479 °C (Mofokeng *et al*., 2012). This behavior was due to the random chain-scission along the main polymer chain after the radical transfer process (An *et al*., 2018). The iPP-g-PVBC copolymer exhibited two distinct degradation steps after moisture loss occurring at 200 -310 °C; the degradation of the grafted PVBC units at 310-350 °C (Song *et al*., 2014) and degradation of the iPP backbone from 385 to 493 °C. The higher onset and maximum degradation temperatures observed from the iPP backbone in the thermogram of the iPP-g-PVBC compared with pristine iPP indicated an improvement of its thermal resistance following the grafting reaction.

The degradation profile of iPP-g-PVBC-TMA-Cl showed an initial 7% weight loss, which can be linked to moisture elimination at 100-114 °C (Mahmoud and Hegazy, 2004). The iPP-g-PVBC-TMA-Cl membrane exhibited a two-step weight loss profile: first was the degradation of the quaternary ammonium group with onset at 170 °C (Sherazi *et al*., 2013; Vengatesan *et al*., 2015), while the second step with onset at 390 °C was the decomposition of the aromatic group of the graft chain (Sherazi *et al*., 2013; Vengatesan *et al*., 2015), which also concurred with the degradation of the iPP backbone. For the iPP-g-PVBC-TOH membrane, an initial weight loss was also recorded due to the removal of the adsorbed water. The initial degradation step with onset at 170 °C can be attributed to the removal of the –CH2N(CH3)3-OH group. The second and third steps, which corresponded to the overlapping degradation profile of the PVBC units and the iPP backbone, were recorded at 390 °C.

3.3.3 Elemental Distributions

The elemental distributions of the pristine iPP, iPP-g-PVBC and iPP-g-PVBC-TMA-OH were identified using EDX analysis. The cross-section maps are shown in Figure 7. The membrane thickness, which could be deduced from the C-elemental maps, increased after the addition of grafted PVBC through the iPP film. The successful grafting through the bulk of the membrane was supported by the Cl elemental map, which clearly showed uniform distribution of Cl atoms in the iPP-g-PVBC. The presence of grafted chains in the inner segments of the membrane is important as it suggests the presence of continuous conducting channels that could transport the OH- ions from the cathode to the anode. The hydroxylated film showed a decreased density of Cl atoms as these were displaced by the OH- groups. The elemental maps, together with the other data presented above, conclusively presented the

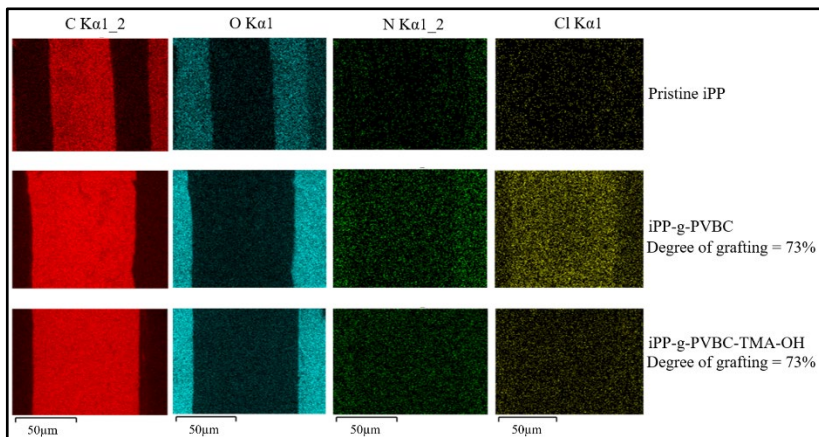successful preparation of AEM through radiation grafting and post-grafting functionalization reactions.

Figure 7. Cross-section SEM-EDX mapping of the of iPP film, iPP-g-PVBC and iPP-g-PVBC-TMA-OH

3.4 IEC

The theoretical and experimental IEC values of the membranes with different degrees of grafting are plotted in Figure 8. The theoretical IEC values were based on the degree of grafting at 100% Da, where each benzyl unit was quaternized with one TMA group.
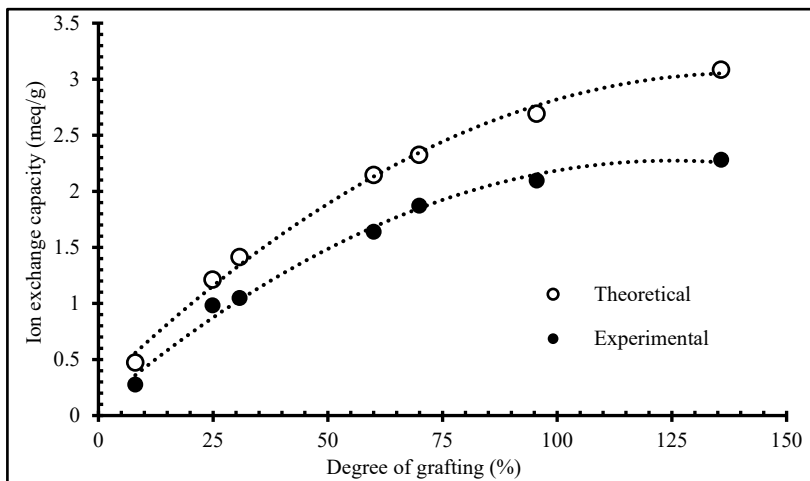

Figure 8. Comparison of the effect of degree of grafting on the theoretical and experimental IEC values of the AEMs

It was shown that IEC increased with increasing degree of grafting as a result of incorporating more functional groups, available for the exchange of OH-ions (Espiritu *et al.*, 2016), to the polymer backbone. The highest IEC (2.28 meq/g) was achieved with the membrane having 136% degree of grafting (ICOH- = 161.01 mS/cm at 60 °C). This IEC value is sufficient to achieve the same proton IC of the commercially available proton electrolyte membrane (Nafion, IC = 0.1 S/cm at 80 °C) which requires > 2.0 mmol/g IEC (Espiritu *et al.*, 2016). The experimental values of the IEC were lower compared with the theoretical values due to the incomplete quaternization of the iPP-g-PVBC as shown in section 3.2 and the incomplete displacement of the Cl- by OH-ions. The lower experimental value of IEC compared with the theoretical value was also observed even in proton exchange membranes (Mazzapioda *et al.*, 2019).

3.5 IC and WU

The conductivity of the AEM must be sufficiently high and selective for the fuel cell to work. The main role of the AEM was to conduct the OH- ions from the cathode to the anode where reduction of oxygen gas and oxidation of fuel occurs (Arges *et al.*, 2010; Sherazi *et al.*, 2013; Dekel, 2018). The OH- ion conductivities of the membranes with different degrees of grafting values are shown in Figures 9a (25 °C) and 9b (60 °C). The conductivities of the membranes in Cl- form are also shown for comparison. Results showed that the ionic conductivities were temperature-dependent – a behavior similar to proton exchange membranes (Sherazi *et al.*, 2013). Higher ionic conductivities were obtained at a higher temperature (60 °C) than the room temperature (25 °C) values. The IC values for iPP-g-PVBC-TMA-OH increased with increasing degree of grafting reaching 162.1 mS/cm (degree of grafting = 96%) and 161.0 mS/cm (degree of grafting = 136%). The slight decrease in the IC of the membrane with a 136% degree of grafting can be ascribed to the excessive swelling suffered by the membrane which affected its conductivity (Arges *et al.*, 2010).

The WU is a property related to the IEC as it is also dependent on the number of available ion-exchange sites. The membranes' WU capacity directly affects the IC and mechanical properties of the membrane (Li *et al.*, 2010; Sherazi *et al.*, 2013). The WU can be measured through the amount of water in the membrane and consequently affects its swelling (Espiritu et al., 2016). The water uptake plots of the chloride and hydroxide forms of the membranes with different degrees of grafting values are shown in Figures 9c (25 °C) and 9d (60 °C).
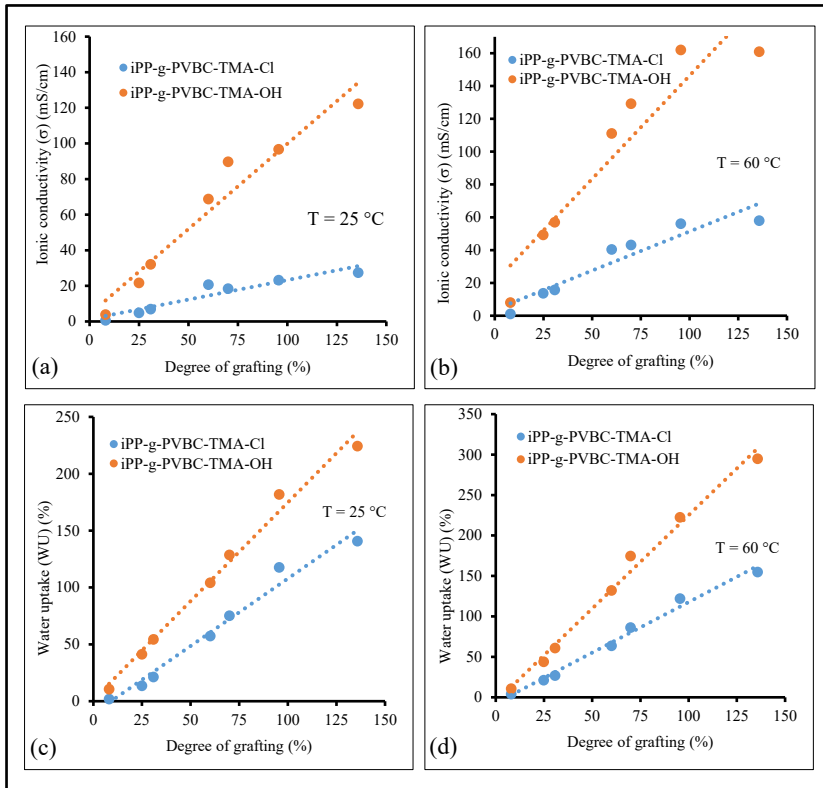
Figure 9. Ionic conductivity plots of chloride and hydroxide forms of the membrane at 25 °C (a) and 60 °C (b) and water uptake plots of chloride and hydroxide forms of the membrane at 25 °C (c) and 60 °C (d)

As expected, a high degree of grafting membranes led to high WU values (Espiritu *et al*., 2016) due to the presence of more ion exchangeable sites brought by the high amount of quaternized grafted PVBC units. Increasing the temperature from 25 to 60 °C did not significantly affect the WU of the membrane in chloride form. On the other hand, a different behavior was observed in the hydroxide form of the membrane, which exhibited an increase in WU with an increase in temperature. The WU of the iPP-g-PVBC-TMA-OH (degree of grafting = 135.73%) measured at 60 °C was excessively high at 295%. Although high WU is needed to attain high conductivity (Sherazi *et al*., 2013), excessive WU resulted in a slight decrease of the IC of the membrane as it affected its mechanical properties. This was evident in the synthesized membranes with the degree of grafting values of > 70% where dimensional changes such as wrinkling and excessive swelling were observed, and these caused the slight decrease in the IC as shown in Figure 9b. The drop

in IC was linked to the reduction of the effective membrane-phase concentration of the fixed charges on the membrane caused by the excessive swelling (Arges *et al*., 2010).

Considering the IC and WU values of the synthesized membranes, a very high degree of grafting was not necessary, and grafted membrane with less than 100% degree of grafting was sufficient. The synthesized AEM with a degree of grafting of 70% (IC = 129.34 mS/cm) exhibited moderate swelling and IEC (1.87 meq/g), thus making it more applicable for fuel cell applications. Also, when compared with other AEMs synthesized using radiation grafting with almost the same degree of grafting, the iPP-g-PVBC-TMA-OH produced higher conductivities even at a lower temperature (Table 1).

Table 1. IC values comparison of iPP-g-PVBC-TMA-OH membrane with varying degrees of grafting with other radiation grafted AEMs

Membrane	Degree of grafting (%)	Temperature (°C)	Hydroxide ion conductivity (mS/cm)
iPP-g-PVBC-TMA-OH	8.0	60.0	8.1
	24.9	60.0	49.3
	69.9	60.0	129.3
	95.5	60.0	162.1
	135.7	60.0	161.0
PE-g-PVBC-TOH (Sherazi *et al*., 2013)	12.7	90.0	47.5
PE-g-PVBC-TOH (Espiritu *et al*., 2016)	71.3	70.0	120.0
ETFE-AEM (Varcoe, 2007)	23.6	30.0	30.0

4. Conclusion

An AEM was successfully prepared through radiation-induced graft polymerization of poly(vinylbenzyl chloride) from isotactic polypropylene film using the pre-irradiation technique. A higher degree of grafting resulted in higher IC, IEC and WU for both forms of the membrane, namely iPP-g-PVBC-TMA-Cl and iPP-g-PVBC-TMA-OH. A balance among the membrane properties was achieved by controlling the degree of grafting. The synthesized

AEM with a degree of grafting of 70% (IEC = 1.87 meq/g) obtained a conductivity of 129.34 mS/cm, which is higher compared with the AEMs from previous studies.

5. Acknowledgement

6. References

Albano, C., Perera, R., Silva, P., & Sánchez, Y. (2006). Characterization of irradiated PEs/PA6 blends. Polymer Bulletin, 57(6), 901-912. https://doi.org/10.1007/s00289-006-0651-y

An, T., Hai, P., Matsukuma, H., & Sugimoto, R. (2018). Surface modification of polypropylene with poly(3-hexylthiophene) via oxidative polymerization. Reactive and Functional Polymers, 122, 167-174. https://doi.org/10.1016/j.reactfunctpolym.2017.12.002

Arges, C.G., Ramani, V., & Pintauro, P.N. (2010). The chalkboard: Anion exchange membrane fuel cells. The Electrochemical Society Interface, 19, 31-35.

Bhardwaj, Y., Tamada, M., Nho, Y.-C., Nasef, M., & Güven, O. (2014). Harmonized protocol for radiation-induced grafting. Retrieved from http://www-naweb.iaea.org/napc/iachem/working_materials/Graftingprotocol.pdf

Bhattacharya, A., & Misra, B.N. (2004). Grafting : A versatile means to modify polymers techniques, factors and applications. Progress in Polymer Science, 29(8), 767-814. https://doi.org/10.1016/j.progpolymsci.2004.05.002

Couture, G., Alaaeddine, A., Boschet, F., & Ameduri, B. (2011). Progress in polymer science polymeric materials as anion-exchange membranes for alkaline fuel cells. Progress in Polymer Science, 36(11), 1521-1557. https://doi.org/10.1016/j.progpolymsci.2011.04.004

Dargaville, T.R., George, G.A., Hill, D.J.T., & Whittaker, A.K. (2003). High energy radiation grafting of fluoropolymers. Progress in Energy and Combustion Science, 28(9), 1355-1376. https://doi.org/10.1016/S0079-6700(03)00047-9

Dekel, D.R. (2018). Review of cell performance in anion exchange membrane fuel cells. Journal of Power Sources, 375, 158-169. https://doi.org/10.1016/j.jpowsour.20 17.07.117

Espiritu, R., Mamlouk, M., & Scott, K. (2016). Study on the effect of the degree of grafting on the performance of polyethylene-based anion exchange membrane for fuel cell application. International Journal of Hydrogen Energy, 41(2), 1120-1133. https://doi.org/10.1016/j.ijhydene.2015.10.108

Fuel Cells Bulletin. (2021). Fuel cell power for Philippines cellular sites. Fuel Cells Bulletin, 8, 7. https://doi.org/10.1016/S1464-2859(09)70252-4

Ghosh, S. (1998). Textile application of molecular spectroscopy. In J. Workman Jr. & A.W. Springsteen (Eds.), Applied spectroscopy: A compact reference for practitioners (pp. 437-457). Massachusetts, United States: Academic Press.

Hoshina, H., Kasai, N., Amada, H., Takahashi, M., Tanaka, K., & Seko, N. (2014). Recovery of scandium from hot spring water with graft adsorbent containing phosphoric groups. Journal of Ion Exchange, 25(4), 248-251. https://doi.org/10.5182/ja ie.25.248

Iojoiu, C., Chabert, F., Mar, M., & Kissi, N.E. (2006). From polymer chemistry to membrane elaboration: A global approach of fuel cell polymeric electrolytes. Journal of Power Sources, 153(2), 198-209. https://doi.org/10.1016/j.jpowsour.2005.05.039

Laura, A., Biancolli, G., Herranz, D., Wang, L., Stehl, G., & Zhang, Z. (2018). ETFE-based anion-exchange membrane ionomer powders for alkaline membrane fuel cells: A first performance comparison of head-group chemistry. Journal of Materials Chemistry A, 6(47), 24330-24341. https://doi.org/10.1002/app.46886

Li, Y.S., Zhao, T.S., & Yang, W.W. (2010). Measurements of water uptake and transport properties in anion-exchange membranes. International Journal of Hydrogen Energy, 35(11), 5656-5665. https://doi.org/10.1016/j.ijhydene.2010.03.026

Lim, T.M., Ulaganathan, M., & Yan, Q. (2015). Advances in membrane and stack design of redox flow batteries (RFBs) for medium- and large-scale energy storage. In C. Menictas, M. Skyllas-Kazacos & T.M. Lim (Eds.), Advances in batteries for medium and large-scale energy storage (pp. 477-507). Sawston, United Kingdom: Woodhead Publishing.

Lopez, G.E.P., Madrid, J.F., & Abad, L.V. (2020). Chromium and cadmium adsorption on radiation-grafted polypropylene copolymers : Regeneration, kinetics, and continuous fixed bed column studies. SN Applied Sciences, 2(3), 1-10. https://doi.org/10.1007/s42452-020-2168-7

Maddah, H. (2016). Polypropylene as a promising plastic: A review. American Journal of Polymer Science, 6(1), 1-11. https://doi.org/10.5923/j.ajps.20160601.01

Madrid, J.F., & Abad, L.V. (2015). Modification of microcrystalline cellulose by gamma radiation-induced grafting. Radiation Physics and Chemistry, 115, 143-147. https://doi.org/10.1016/j.radphyschem.2015.06.025

Madrid, J.F., Barsbay, M., Abad, L., & Güven, O. (2016). Grafting of N,N-dimethylaminoethyl methacrylate from PE/PP nonwoven fabric via radiation-induced RAFT polymerization and quaternization of the grafts. Radiation Physics and Chemistry, 124, 145-154. https://doi.org/10.1016/j.radphyschem.2016.01.004

Madrid, J.F., Cabalar, P.J.E., & Abad, L.V. (2018). Radiation-induced graft polymerization of acrylic acid and glycidyl methacrylate onto abaca/polyester nonwoven fabric. Journal of Natural Fibers, 15, 625-638. https://doi.org/10.1080/15440478.2017.1349713

Mahmoud, M., & Güven, O. (2012). Radiation-grafted copolymers for separation and purification purposes: Status, challenges and future directions. Progress in Energy and Combustion Science, 37(12), 1597-1656. https://doi.org/10.1016/j.progpolymsci.2012.07.004

Mahmoud, M., & Hegazy, E.A. (2004). Preparation and applications of ion exchange membranes by radiation-induced graft copolymerization of polar monomers onto non-polar films. Journal of Macromolecular Science, Part A, 29, 499-561. https://doi.org/10.1016/j.progpolymsci.2004.01.003

Mazzapioda, L., Panero, S., & Navarra, M.A. (2019). Polymer electrolyte membranes based on nafion and a superacidic inorganic additive for fuel cell applications. Polymers, 11(5), 914. https://doi.org/10.3390/polym11050914

Merle, G., Wessling, M., & Nijmeijer, K. (2011). Anion exchange membranes for alkaline fuel cells : A review. Journal of Membrane Science, 377, 1-35. https://doi.org/10.1016/j.memsci.2011.04.043

Mofokeng, J.P., Luyt, A.S., Tábi, T., & Kovács, J. (2012). Comparison of injection moulded, natural fibre-reinforced composites with PP and PLA as matrices. Journal of Thermoplastic Composite Materials, 25(8), 927-948. https://doi.org/10.1177/0892705711423291

Page, K.A., & Rowe, B.W. (2012). An overview of polymer electrolyte membranes for fuel cell applications. In K.A. Page, C.L. Soles & J. Runt (Eds.), Polymers for energy storage and delivery: Polyelectrolytes for batteries and fuel cells (pp. 147-164). Washington, D.C., United States: American Chemical Society.

Park, J., Takayama, T., Asano, M., Maekawa, Y., & Kudo, K. (2013). Graft-type polymer electrolyte membranes for fuel cells prepared through radiation-induced graft polymerization into alicyclic polybenzimidazoles. Polymer, 54(17), 4570-4577. https://doi.org/10.1016/j.polymer.2013.06.042

Pomicpic, J., Dancel, G.C., Cabalar, P.J., & Madrid, J. (2020). Methylene blue removal by poly(acrylic acid)-grafted pineapple leaf fiber/polyester nonwoven fabric adsorbent and its comparison with removal by gamma or electron beam irradiation. Radiation Physics and Chemistry, 172, 108737. https://doi.org/10.1016/j.radphyschem.2020.108737

Ramirez, S., & Paz, R. (2018). Hydroxide transport in anion-exchange membranes for alkaline fuel cells. In S. Karakuş (Ed.), New trends in ion exchange studies (pp. 51-70). London, United Kingdom: IntechOpen Limited.

Seko, N., Ueki, Y., Hoshina, H., & Tamada, M. (2007). Preparation of graft adsorbent having amine groups and its Au (III) adsorption performance Japan atomic. Journal of Ion Exchange, 18(4), 232-235. https://doi.org/10.5182/jaie.18.232

Sherazi, T.A., Ahmad, S., Kashmiri, M.A., & Guiver, M.D. (2008). Radiation-induced grafting of styrene onto ultra-high molecular weight polyethylene powder and subsequent film fabrication for application as polymer electrolyte membranes: I. Influence of grafting conditions. Journal of Membrane Science, 325(2), 964-972. https://doi.org/10.1016/j.memsci.2008.09.028

Sherazi, T.A., Yong Sohn, J., Moo Lee, Y., & Guiver, M.D. (2013). Polyethylene-based radiation grafted anion-exchange membranes for alkaline fuel cells. Journal of Membrane Science, 441, 148-157. https://doi.org/10.1016/j.memsci.2013.03.053

Song, J., Lee, S., Woo, H., Sohn, J., & Shin, J. (2014). Thermal behavior of poly(vinylbenzyl chloride) grafted poly(ethylene-co-tetrafluoroethylene) films. Journal of Polymer Science Part B: Polymer Physics, 52(7), 517-525. https://doi.org/10.1002/polb.23445

Ueki, Y., Mohamed, N.H., Seko, N., & Tamada, M. (2011). Rapid biodiesel fuel production using novel fibrous catalyst synthesized by radiation-induced graft polymerization. International Journal of Organic Chemistry, 1(2), 20-25. https://doi.org/10.4236/ijoc.2011.12004

Ueki, Y., Saiki, S., Shibata, T., Hoshina, H., Kasai, N., & Seko, N. (2014). Optimization of grafted fibrous polymer as a solid basic catalyst for biodiesel fuel production. International Journal of Organic Chemistry, 4(2), 91-105. https://doi.org/10.4236/ijoc.2014.42011

Varcoe, J.R. (2007). Investigations of the ex situ ionic conductivities at 30 °C of metal-cation-free quaternary ammonium alkaline anion-exchange membranes in static atmospheres of different relative humidities. Physical Chemistry Chemical Physics, 9(12), 1479-1486. https://doi.org/10.1039/b615478f

Varcoe, J.R., & Slade, R.C.T. (2006). An electron-beam-grafted ETFE alkaline anion-exchange membrane in metal-cation-free solid-state alkaline fuel cells. Electrochemistry Communications, 8(5), 839-843. https://doi.org/10.1016/j.elecom.2006.03.027

Varcoe, J.R., Slade, R.C.T., Wright, G.L., & Chen, Y. (2006). Steady-state dc and impedance investigations of H_2/O_2 alkaline membrane fuel cells with commercial Pt/C, Ag/C, and Au/C cathodes. The Journal of Physical Chemistry B, 2(3), 21041-21049.

Vengatesan, S., Santhi, S., Sozhan, G., Ravichandran, S., Davidson, J., & Vasuden, S. (2015). Novel cross-linked anion exchange membrane based on hexaminium functionalized poly(vinylbenzyl chloride). RSC Advances, 5, 27365-27371.

Yang, C., Liu, L., Huang, Y., Dong, J., & Li, N. (2019). Anion-conductive poly(2,6-dimethyl-1,4-phenylene oxide) grafted with tailored polystyrene chains for alkaline fuel cells. Journal of Membrane Science, 573, 247-256. https://doi.org/10.1016/j.memsci.2018. zz12.013

Zabbaruddin, N.H., Mohamed, N.H., Abdullah, L. C., Tamada, M., Ueki, Y., Seko, N., & Choong, T.S.Y. (2019). Palm oil-based biodiesel synthesis by radiation-induced kenaf catalyst packed in a continuous flow system. Industrial Crops and Products, 136, 102-109. https://doi.org/10.1016/j.indcrop.2019.04.069

Zhang, Z. (2019). Highly conductive anion exchange membranes based on one-step benzylation modification of poly(ether ether ketone). Journal of Membrane Science, 574, 205-211. https://doi.org/10.1016/j.memsci.2018.12.080

Zheng, Y., Colón, L.N.I., Hassan, N.U., Williams, E.R., Stefik, M., Lamanna, J.M., Hussey, D.S., & Mustain, W.E. (2021). Effect of membrane properties on the carbonation of anion exchange membrane fuel cells. Membranes, 11(2), 1-14. https://doi.org/10.3390/membranes11020102